Cavity-enhanced second-harmonic generation in strongly scattering nonlinear media

Yanqi Qiao, Fangwei Ye, Yuanlin Zheng, and Xianfeng Chen*

State Key Laboratory of Advanced Optical Communication Systems and Networks, School of Physics and Astronomy, Shanghai Jiao Tong University, Shanghai 200240, China and Key Laboratory for Laser Plasma (Ministry of Education), Collaborative Innovation Center of IFSA (CICIFSA), Shanghai Jiao Tong University, Shanghai 200240, China

(Received 27 April 2018; published 30 April 2019)

Light interaction with random linear or nonlinear media is always an interesting scheme to study Anderson localization of photons and phase-matching-free nonlinear optics. Here, a cavity-enhanced second-harmonic generation (SHG) process in a random nonlinear material was experimentally demonstrated. Compared to the conventional random laser action based on the photoluminescence (PL) effect, this cavity-enhanced SHG indicates a possible Anderson localization of the nonlinear signals by ring cavities and widens the response wave band due to the flexible frequency conversion in the nonlinear process. The combination of the random cavity scheme and the random quasi-phase-matching scheme will provide us another way to break phase-matching limitations, with locally high conversion efficiency. This work suggests important progress on nonlinear Anderson localization and indicates many potential applications, such as a band-tunable random nonlinear laser, phase-matching-free nonlinear optics, and even focusing or imaging through random nonlinear media with a nice conversion efficiency.

DOI: 10.1103/PhysRevA.99.043844

I. INTRODUCTION

Anderson localization of photons and the interaction between light and random media have always attracted both theoretical and experimental physicists [1–3]. Over the past decades, a random photoluminescence (PL) laser action has provided a new way to understand this scheme, where the "ring cavity" formed by recurrent scattering was proven to achieve light confinement and laser emission, instead of the standard optical cavities, such as Fabry-Perot (FP) resonators, whispering-gallery-mode resonators, and photonic crystal cavities [4–10]. Recently, a random Raman laser was also demonstrated in a three-dimensional system via the stimulated Raman scattering (SRS) effect [11]. However, this work indicated no cavity confinement or coherent feedback responsible for the bright emission. In general, the previous random laser scheme provided a new laser mode to achieve a local signal enhancement, but it needed an active medium with a good photoresponse via a four-level or Raman-level transition process [11,12]. The response wave band was also limited by the inherent energy-level structure of the material.

Phase matching (PM) and quasi phase matching (QPM) are always known as the hard conditions for high conversion efficiency in nonlinear optics [13]. People have come up with many ingenious methods to break that limitation, such as zero-index metamaterial [14] and a random quasi-phase-matching (RQPM) scheme [15–17], using nonlinear materials with randomized domain structure to achieve nonlinear emission. However, there are many drawbacks with these methods, such as the complicated sample design and low conversion efficiency. Fortunately, a possible combination of random laser and RQPM was introduced here for a locally high efficiency in nonlinear conversion or even Anderson localization of nonlinear photons, because both of them occurred in the random structures. Furthermore, a random fiber laser [18] and a feedback-based wave-front shaping method [19–23] were demonstrated to be valid in random nonlinear optics, providing possible ways to transmit the signals directionally.

In this paper, we experimentally demonstrated the cavity-enhanced SHG in superfine lithium niobate (LN) powder, which proved a possible confinement of the nonlinear signals and locally high conversion efficiency in the random cavity. This is a unique kind of random SHG laser action, and it also marks important progress on studying the nonlinear Anderson localization because traditional nonlinear material is usually not laser gain medium for stimulated radiation. At the same time, this cavity-enhanced SHG widens the response wave band due to the flexible frequency conversion in a virtual state-based nonlinear process. First of all, a coherent backscattering (CBS) experiment was carried out to describe the scattering strength inside our samples. In the SHG enhancing experiments, extremely sharp peaks were observed emerging or vanishing in the broad SH spectra with the increasing of the fundamental wave (FW) intensity. When considering the increased intensity of one SH mode, we found a deviation on the normally quadratic relation of FW and SH, similar to the threshold behavior in random lasers. Finally, more comparison and verification tests were carried out to further support our argument experimentally.

II. A SIMPLIFIED THEORETICAL DESCRIPTION

The concept of the cavity-enhanced SHG in a strong scattering medium was illustrated in Fig. 1. When a broadband FW laser entered the sample and scattered randomly,

*xfchen@sjtu.edu.cn

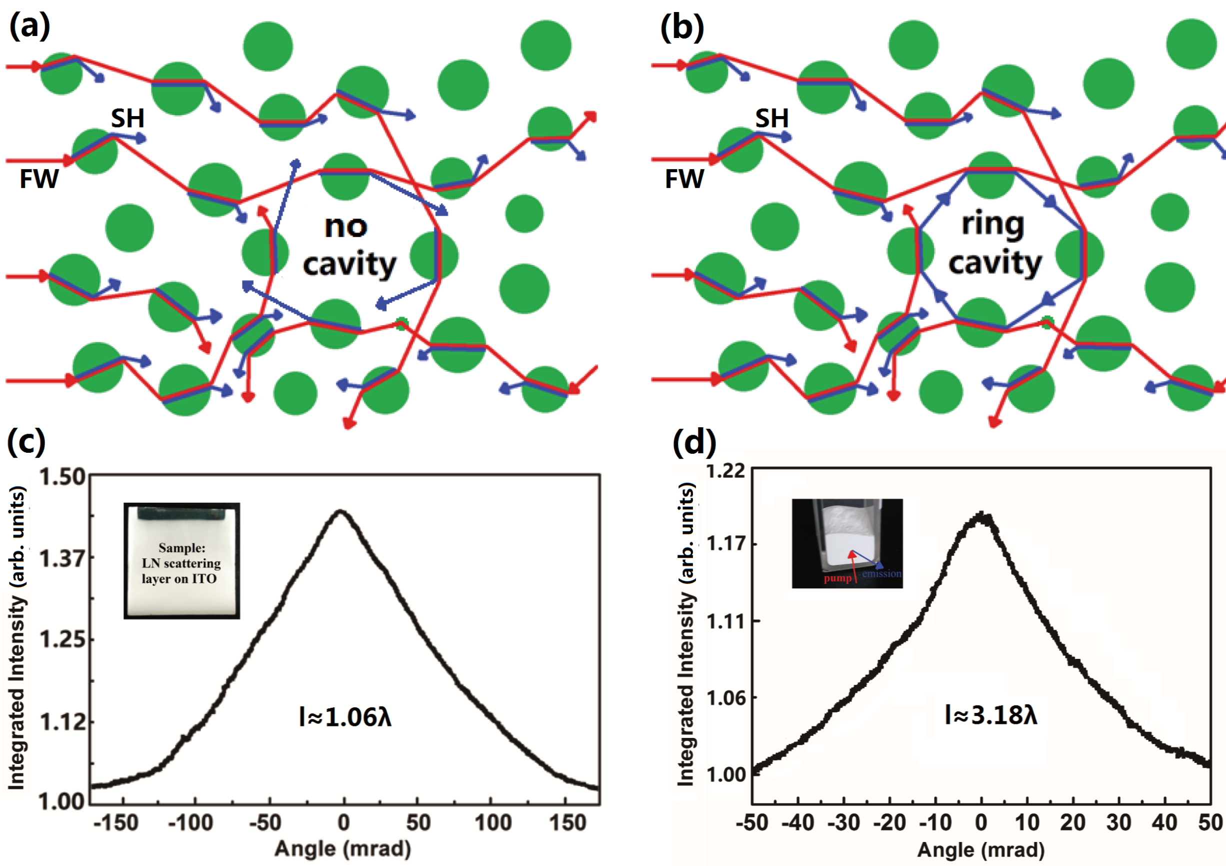

FIG. 1. (a) The SH signals as well as the FW laser were generated and scattered from nonlinear powder with no obvious enhancement. (b) The SH signals formed a ring cavity at a certain pump intensity, showing a local enhancement. (c), (d) Coherent backscattering cones from LN-ITO film and loosely packed LN powder at a wavelength of 405 nm, respectively.

a second-order nonlinear process occurred in every pumped LN particle. These particles became SH sources, radiating double-frequency light in various directions. Both the FW and SH signals scattered from nonlinear powder were disorganized at first without any obvious enhancement [Fig. 1(a)]. According to the third-order nonlinear property of LN powder, the refractive index of the FW would change with the pump intensity changing, especially noteworthy under a high-power pump. This relation is known as

$$n = n_0 + \Delta n(|E|^2),$$

where $\Delta n(|E|^2)$ represents the FW refractive index changing based on its intensity. Thus, the scattering of FW and SH was totally different inside the powder when the pump intensity was changing. It is usually reasonable to increase the pump intensity instead of decreasing it as changing, considering a stronger signal for easier detection and a larger n for stronger scattering. The possibility of forming a ring cavity would be higher with the scattering stronger, so it is easier to find the cavity behavior in the SH emission macroscopically by increasing the FW intensity, as shown in Fig. 1(b).

III. EXPERIMENTAL DEMONSTRATION

In our experiment, LN nanocrystal powder was applied as the random scattering medium. It was prepared by a solid-state reaction method, using niobium pentoxide (Nb_2O_5) and lithium acetate dihydrate ($C_2H_3O_2Li \cdot 2H_2O$) as the reactants. The obtained particles have an average size of 300 nm under scanning electron microscopy imaging (see Fig. 2, inset2). The powder was then deposited onto an indium–tin oxide (ITO) coated glass substrate by an electrophoresis method [4,24], with the inset in Fig. 1(c) showing a photograph of the sample. The LN powder film has the size of 30×30 mm^2, with a thickness of around 100 μm. To characterize the scattering strength of the film, a CBS experiment [25–27] was carried out at a probe wavelength of 405 nm (output of a violet diode laser). The measured backscattering cones of the LN-ITO film and a loosely packed LN powder structure in a 10×10 mm^2 cuvette [Fig. 1(d), inset] are shown in Figs. 1(c) and 1(d), respectively. From the full width at half maximum (FWHM) of the cones, the scattering mean free paths were estimated to be $l \cong 1.06\lambda$ and $l \cong 3.18\lambda$, respectively, according to the formula $\theta \approx \lambda/(2\pi l)$ [4,27].

In the experimental setup as shown in Fig. 2, the light source was a Ti:sapphire femtosecond regenerative amplifier system (50-fs duration, 1-kHz repetition rate). The center wavelength of the FW laser was about 793.5 nm, as shown in inset 1. A tunable attenuator was applied to control the pump intensity. A filter system before the spectroscopy was set to reject the high-power pump. All spectra were measured by a high-resolution optical spectrometer (SR-500, Andor,

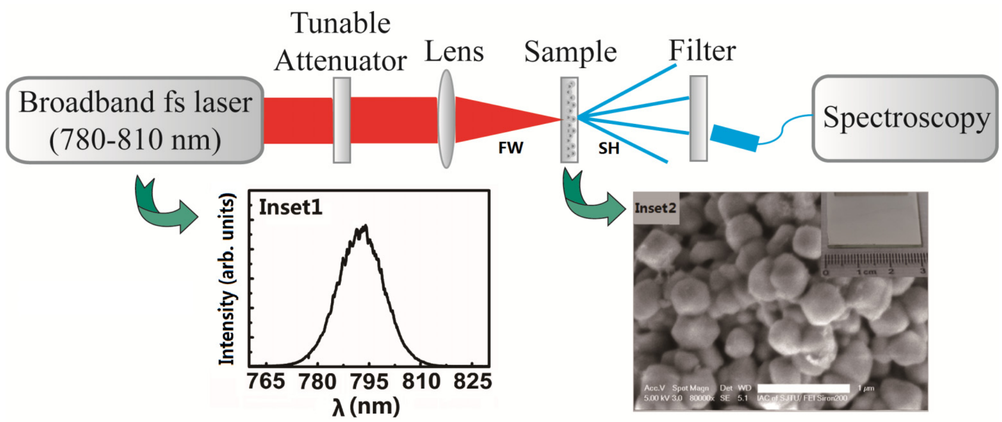

FIG. 2. The experimental setup for random cavity-enhanced SHG process. Inset 1: The original FW spectrum centered at 793.5 nm. Inset 2: LN particles under the scanning electron microscope (scale bar: 1 μm).

resolution 0.1 nm). The pump position and the detecting angle were determined randomly for generality. First of all, the LN-ITO film with a higher scattering ability was applied in the setup. A typical result of the SH spectrum was shown in Fig. 3(a). Obviously, the SH spectrum was changing with the increasing of the FW intensity from 4.5 to 79.1 mW/mm^2. There were three typical sharp peaks (FWHM $\approx$1 nm) emerging in the spectrum at 79.1 mW/mm^2 pumping (1.58 GW/mm^2 in peak intensity). They were at 394.0 nm, 395.5 nm (①), and 397.5 nm (②), respectively. It is worth mentioning that the FW spectrum remained similar under the same power steps except for some fluctuations (no similar peak) as shown in Fig. 3(b), proving that the confinement was formed by SH signals, not the FW laser. It is easy to understand because the Mie scattering theory illuminates that the higher-frequency light encounters stronger scattering in the turbid medium.

It is necessary to analyze the FW and SH relation in the peak wavelengths for a further understanding of the result, similar to the threshold analysis in random PL and Raman lasers. Firstly, the integrated SH intensity from 39 to –405 nm was power fitted with the pump intensity as a reference [Fig. 3(c)], with the expression of $I_{SH} = A(I_{FW} - I_o)^P$, where I_o represents the cutoff intensity on the x axis and P represents the enhancement factor. According to traditional second-order nonlinear optics, the relation between SH and FW should be perfect quadratic; that means $P = 2$. However, we arrived at $P = 1.81$, which was not a perfect quadratic relation because of the complex absorption and strong scattering inside the particles [28]. Then, we got $P = 2.04$ and $P = 1.93$ at positions ① and ②, respectively, based on the same power fitting [Figs. 3(d) and 3(e)]. This deviation was as expected and proved the local SH enhancement at some certain wavelengths. For a comparison, a randomly selected position ③ was also fitted and showed $P = 1.64$ [Fig. 3(f)], which is lower than the integrated value as expected and even much lower than 2, indicating a possible inhibitory effect on this frequency conversion caused by those cavities.

IV. MORE COMPARISON AND VERIFICATION TESTS

It is a difficult task to carry out an in-depth study theoretically with the combination of nonlinear wave equation and random cavity theory. Instead, more comparison and verification tests were carried out to further support the argument experimentally. First of all, the angle and film thickness dependences of the cavity-enhanced SHG were revealed in Fig. 4. Three different detecting angles, 0°, 30°, and 60°, were applied but the film thickness was kept to 100 μm, as shown in Figs. 4(a)–4(c). All typical SH enhancements were observed at the FW pump intensity around $18 - 38$ mW/mm^2, whatever detecting angle was applied. This result proved that the cavity-enhanced SHG has no directionality and the interaction property inside the sample is independent of the detecting angle. However, the whole SH intensity decreased with the increasing of the detecting angle due to the scattering cross-section nature. It is worth mentioning that applying different pump angles should produce similar behavior due to the isotropy of the powder film. Figures 4(a), 4(d), and 4(e) show the film thickness dependence with another two different samples, 50 and 200 μm, fabricated by different depositing times. The pump power for a typical SH enhancement decreased with the increasing of the film thickness as expected, because the interaction length increased relatively with the film thickness, which increased the possibility of forming the cavity. However, the film thickness had a limitation due to the transmittance of the signals.

Another comparison experiment was also carried out with the LN powder loosely packed into a 10×10 mm^2 cuvette [Fig. 1(d), inset] applied in the setup, indicating a weaker light scattering strength in the sample. Figure 5(a) shows a typical series of SH spectra at various pump intensities in the reflecting direction. These spectra enhanced with the pump increasing as expected but no similar sharp peak was observed. Figure 5(b) shows the integrated SH intensity as a function of the pump intensity. A power function was applied to fit the experimental data, arriving at $P = 1.82$. It was similar to the previous result but no obvious derivation of P occurred at any certain wavelength. In fact, one may expect the same SH enhancing process in loosely packed LN powder with much higher pump intensity or additional light confinement, according to the theoretical and experimental results of the random lasers in weakly scattering systems [18,29]. However, the spectrum and the relation between SH and FW intensity was maintained during our experiment with the pump power

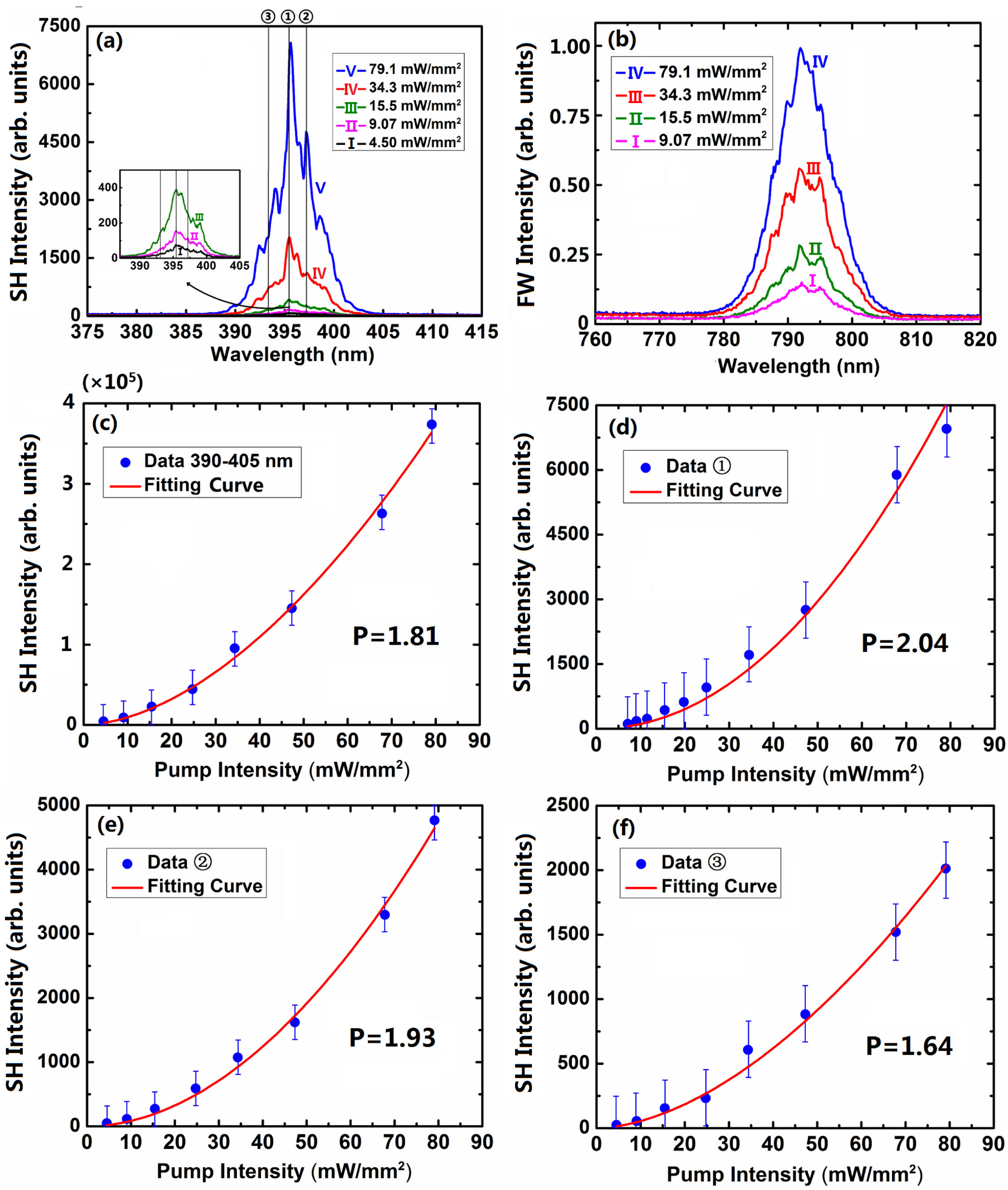

FIG. 3. (a) A typical result of the SH spectrum with some peaks under certain pump power. (b) The FW spectrum under the same power steps with no obvious peak. (c) The integrated SH intensity from 390 to 405 nm fitted with the pump intensity. (d)–(f) SH intensity at different wavelengths fitted with the pump intensity.

increasing until the sample damage threshold, proving the absence of cavity-enhancing process.

To further confirm our argument, the same experiment was conducted on the LN-ITO system except that one surface of the ITO glass was frosted to rule out the possibility of an ITO glass formed FP cavity (thickness: 1 mm). This sample had no smooth surface, so there would be no FP cavity contributing to the SH enhancing [as shown in Fig. 5(c), inset]. An expected result was shown in Fig. 5(c). Besides, one particle serving as the cavity (something like a microcavity or nanocavity) or two particles serving as the resonators (something like a FP cavity) were considered as special cases and included in our scheme.

The stability of the scheme was confirmed by a repeated measurement while pumping at the same position and detecting at the same emission angle. After increasing the pump intensity and getting the emission spectra, we cut the pump power off and reincreased it repeatedly at different time intervals. The spectra were found the same as expected. It is also worth mentioning that we usually increase the pump

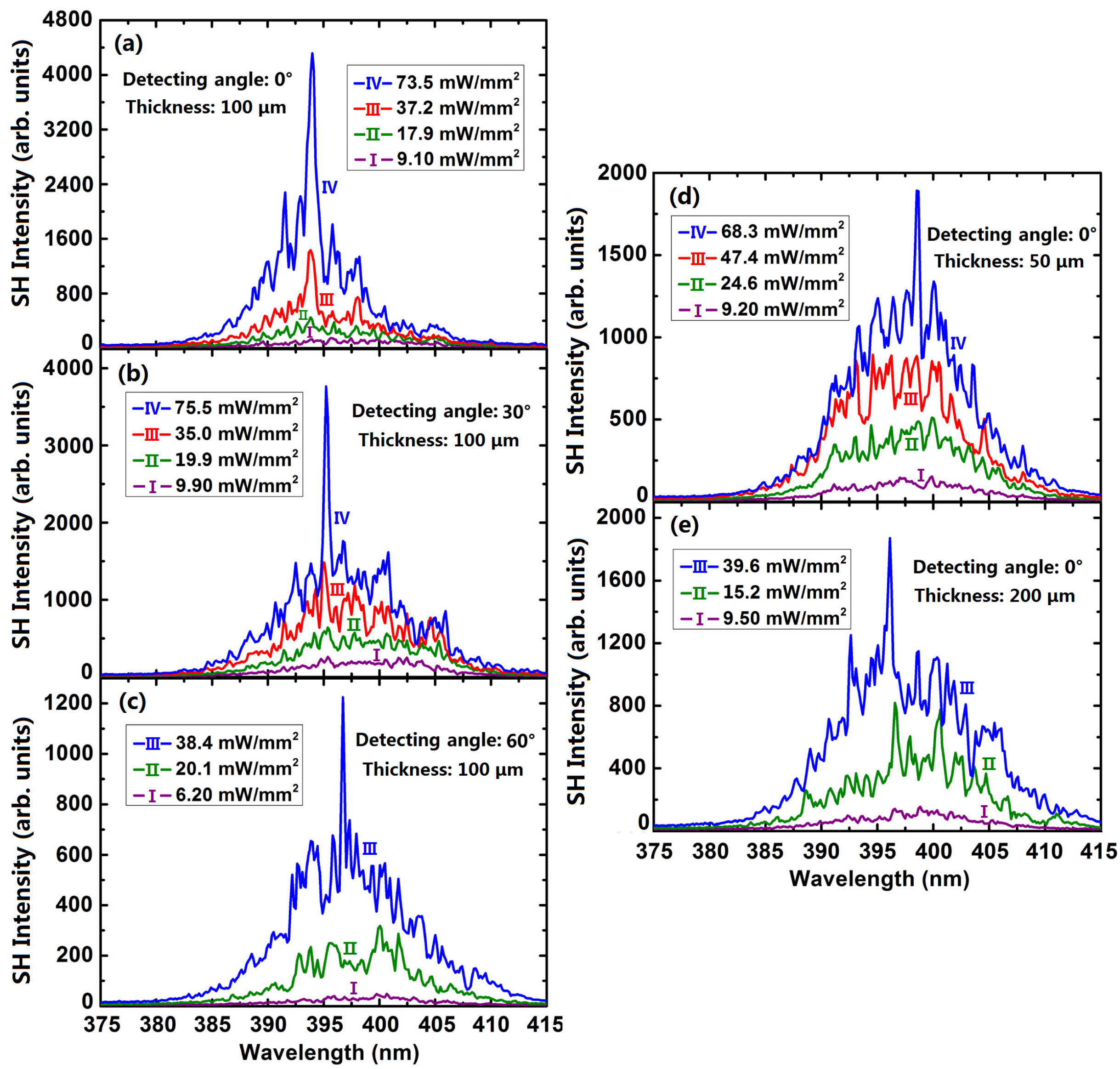

FIG. 4. (a)–(c) the detecting angle dependence of the cavity-enhanced SHG with the film thickness kept to 100 μm. (d), (e) the film thickness dependence of the cavity-enhanced SHG with the pump and detecting angle kept to 0°.

intensity instead of decreasing it to change the scattering path because higher pump energy will cause higher signal power and the scattering strength, leading to a better experimental result. In fact, decreasing the pump energy should also be valid for the cavity-enhancing scheme based on third-order nonlinear theory, but it is not easy to observe. Instead, we found a peak vanishing behavior when increasing the pump energy, which demonstrated the same scheme as the pump decreasing. A typical result was shown in Fig. 5(d), with the film thickness 200 μm. The SH peak at 398.2 nm emerging at around 22.5 mW/mm^2 vanished at 68.3 mW/mm^2 and another peak at 397.5 nm emerged instead. Both the repetition and more peak vanishing (emerging) results can be observed in the video in the Supplemental Material [30]. At the beginning of the video, we increased the pump intensity and observed several peaks' competition on the spectrum. The peak height and shape were also changing during the process. Finally, many peaks vanished and only one of them survived at the largest pump. Then we cut off the pump power and repeat this process, getting the same result as expected.

V. DISCUSSION AND CONCLUSION

In our experimental design, the LN particle was chosen for its large second-order susceptibility and high refractive index ($n \approx 2.2$) for strong scattering. The average size of the particles is much smaller than the SH coherent length L_c in LN crystal (L_c is about several microns), which ensures the maximum emission of every single SH source. Other nonlinear processes [13], such as third-harmonic generation (THG), four-wave mixing (FWM), and coherent anti-Stokes Raman scattering (CARS), etc., are also expected to behave the same in random systems with proper configurations.

In conclusion, we have observed the cavity-enhanced SHG process in superfine LN powder, which shows important progress on the Anderson localization of the nonlinear

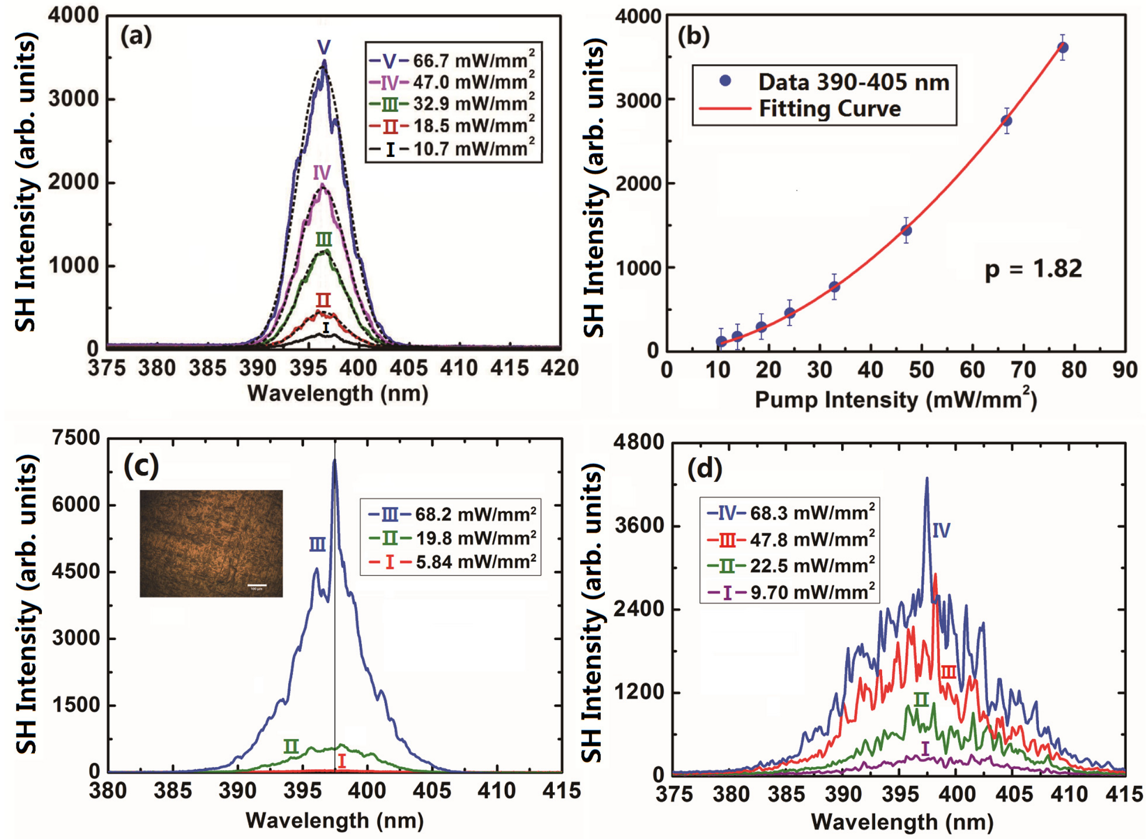

FIG. 5. (a) Typical SH emission spectra of loosely packed LN powder at similar pump intensity steps. (b) The integrated SH intensity from (a) fitted with the pump intensity. (c) A similar SH spectra result from LN-ITO film except for a frosted surface of the ITO glass (scale bar: 100 μm) (d) A typical result to confirm the peak vanishing behavior with a film thickness of 200 μm.

signals. The sharp peaks emerging or vanishing in the broad SH spectra and the *P* derivation characteristics demonstrate the SH confinement directly. The detecting angle and film thickness dependence of the cavity-enhanced SHG were also demonstrated. Some comparison and verification tests were further carried out to support our argument. Compared to conventional random PL laser action and RQPM, the combination will widen the response wave band due to the flexible frequency conversion in nonlinear processes and provide us another possible way to break phase-matching limitations, with locally high conversion efficiency. It is also attractive that a fiber or a feedback-based wave-front shaping method can transmit the random signals directionally, indicating many interesting topics in the future, such as a band-tunable random nonlinear laser and focusing or imaging through random nonlinear media with a nice conversion efficiency [22,31–33].

ACKNOWLEDGMENTS

This work is supported in part by the National Key R&D Program of China (Grant No. 2017YFA0303700), the National Natural Science Foundation of China (NSFC) (Grant No. 11734011), and the Foundation for Development of Science and Technology of Shanghai (Grant No. 17JC1400400).

[1] D. S. Wiersma, P. Bartolini, A. Lagendijk, and R. Righini, Nature (London, UK) **390**, 671 (1997).
[2] E. V. Makeev and S. E. Skipetrov, Opt. Commun. **224**, 139 (2003).
[3] V. A. Mel'nikov, L. A. Golovan, S. O. Konorov, D. A. Muzychenko, A. B. Fedotov, A. M. Zheltikov, V. Yu. Timoshenko, and P. K. Kashkarov, Appl. Phys. B **79**, 225 (2004).
[4] H. Cao, Y. G. Zhao, S. T. Ho, E. W. Seelig, Q. H. Wang, and R. P. H. Chang, Phys. Rev. Lett. **82**, 2278 (1999).
[5] C. Vanneste and P. Sebbah, Phys. Rev. Lett. **87**, 183903 (2001).
[6] S. Mujumdar, M. Ricci, R. Torre, and D. S. Wiersma, Phys. Rev. Lett. **93**, 053903 (2004).
[7] J. Andreasen, A. A. Asatryan, L. C. Botten, M. A. Byrne, H. Cao, L. Ge, L. Labonté, P. Sebbah, A. D. Stone, H. E. Türeci, and C. Vanneste, Adv. Opt. Photonics **3**, 88 (2011).
[8] D. S. Wiersma, Nat. Phys. **4**, 359 (2008).
[9] A. Tulek, R. C. Polson, and Z. V. Vardeny, Nat. Phys. **6**, 303 (2010).
[10] K. J. Vahala, Nature (London, UK) **424**, 839 (2003).
[11] B. H. Hokr, J. N. Bixler, M. T. Cone, J. D. Mason, H. T. Beier, G. D. Noojin, G. I. Petrov, L. A. Golovan, R. J. Thomas, B. A. Rockwell, and V. V. Yakovlev, Nat. Commun. **5**, 4356 (2014).

[12] X. Jiang and C. M. Soukoulis, Phys. Rev. Lett. **85**, 70 (2000).
[13] R. W. Boyd, *Nonlinear Optics* (Academic, New York, 2008).
[14] H. Suchowski, K. O'Brien, Z. J. Wong, A. Salandrino, X. Yin, and X. Zhang, Science **342**, 1223 (2013).
[15] M. Baudrier-Raybaut, R. Haidar, P. Kupecek, P. Lemasson, and E. Rosencher, Nature (London, UK) **432**, 374 (2004).
[16] R. Fischer, S. M. Saltiel, D. N. Neshev, W. Krolikowski, and Y. S. Kivshar, Appl. Phys. Lett. **89**, 191105 (2006).
[17] S. Stivala, A. C. Busacca, A. Pasquazi, R. L. Oliveri, R. Morandotti, and G. Assanto, Opt. Lett. **35**, 363 (2010).
[18] Z. Hu, Q. Zhang, B. Miao, Q. Fu, G. Zou, Y. Chen, Y. Luo, D. Zhang, P. Wang, H. Ming, and Q. Zhang, Phys. Rev. Lett. **109**, 253901 (2012).
[19] I. M. Vellekoop and A. P. Mosk, Opt. Lett. **32**, 2309 (2007).
[20] J. H. Park, C. Park, H. Yu, J. Park, S. Han, J. Shin, S. H. Ko, K. T. Nam, Y. H. Cho, and Y. Park, Nat. Photonics **7**, 454 (2013).
[21] C. Park, J.-H. Park, C. Rodriguez, H. Yu, M Kim, K. Jin, S. Han, J. Shin, S. H. Ko, K. T. Nam, Y.-H. Lee, Y.-H. Cho, and Y. Park, Phys. Rev. Lett. **113**, 113901 (2014).
[22] Y. Qiao, Y. Peng, Y. Zheng, F. Ye, and X. Chen, Opt. Lett. **42**, 1895 (2017).
[23] Y. Qiao, Y. Peng, Y. Zheng, F. Ye, and X. Chen, Opt. Lett. **43**, 787 (2018).
[24] B. S. Jeon, J. S. Yoo, and J. D. Lee, J. Electrochem. Soc. **143**, 3923 (1996).
[25] M. P. Van Albada and A. Lagendijk, Phys. Rev. Lett. **55**, 2692 (1985).
[26] P. E. Wolf and G. Maret, Phys. Rev. Lett. **55**, 2696 (1985).
[27] P. C. de Oliveira, A. E. Perkins, and N. M. Lawandy, Opt. Lett. **21**, 1685 (1996).
[28] S. Faez, P. M. Johnson, D. A. Mazurenko, and A. Lagendijk, J. Opt. Soc. Am. B **26**, 235 (2009).
[29] C. Vanneste, P. Sebbah, and H. Cao, Phys. Rev. Lett. **98**, 143902 (2007).
[30] See Supplemental Material at http://link.aps.org/supplemental/10.1103/PhysRevA.99.043844 for a video showing the repetition and more peak vanishing (emerging) results.
[31] O. Katz, E. Small, Y. Bromberg, and Y. Silberberg, Nat. Photonics **5**, 372 (2011).
[32] O. Katz, E. Small, Y. Guan, and Y. Silberberg, Optica **1**, 170 (2014).
[33] P. Lai, L. Wang, J. W. Tay, and L. V. Wang, Nat. Photonics **9**, 126 (2015).